

# Ultrasound promoted synthesis, characterization and computational studies of some thiourea derivatives

Felix Odame <sup>a, b, \*</sup>, Eric C. Hosten <sup>b</sup>, Kevin Lobb <sup>c</sup>, Zenixole Tshentu <sup>b</sup>

<sup>a</sup> Department of Basic Sciences, University of Health and Allied Sciences PMB 31, Ho, Ghana

<sup>b</sup> Department of Chemistry, Nelson Mandela University, P.O. Box 77000, Port Elizabeth, 6031, South Africa

<sup>c</sup> Department of Chemistry, Rhodes University, P.O. Box 94, Grahamstown, 6140, South Africa

## ARTICLE INFO

### Article history:

Received 26 December 2019

Received in revised form

9 April 2020

Accepted 19 April 2020

Available online 24 April 2020

### Keywords:

Thione

Benzoyl chloride

Benzoyl isothiocyanate

HOMO-LUMO

## ABSTRACT

Synthesis of some thiourea derivatives have been achieved by using ultrasound, the compounds have been characterised using IR, NMR, GC-MS and elemental analysis. The single crystal X-ray structure of *N*-[(benzyloxy)methanethiyl]benzamide (**IV**), 1-benzoyl-3-(2-hydroxyethyl)thiourea (**V**) and 3-benzoyl-1-(1-benzylpiperidin-4-yl)thiourea (**VI**) has been presented and the bond lengths and bond angles contrasted with computed results. The HOMO and LUMO energy levels as well as the global chemical reactivity descriptors of the compounds have also been computed and discussed. Two conformers were obtained for compounds **IV** to **VI** in the molecular Electrostatic potential and the vibrational frequency computations and these have been discussed.

© 2020 Elsevier B.V. All rights reserved.

## 1. Introduction

Ultrasonic irradiation has been used in the synthesis of a number of compounds [1–3]. A reaction between different primary amines, 2,5-hexanedione and dialkyl, diheteroaryl, or diaryl diselenides, have been carried out using catalytic amounts of copper iodide under ultrasonic irradiation [1]. The synthesis of pyrimidine-2-thione have been achieved by the reaction of chalcones and thiourea under conventional and ultrasonic conditions with ultrasound promoted reactions giving higher [2]. 3,4-Dihydropyrimidin-2(1*H*)-ones and thiones derivatives have been synthesized by the condensation of  $\beta$ -dicarbonyl compounds, urea/thiourea and aromatic aldehydes using Dendrimer-PWAn as a nanocatalyst under ultrasonic irradiation [3].

A solvent-free 3-component one-pot reaction between 2,6-diaminopyridine or 1,2-diaminobenzene and  $\text{NH}_4\text{SCN}$  with subsequent addition of an aryl chloride afforded bis-1-(aroyl)-3-(arylyl) thioureas in excellent yields. The thiocyanate derivatives were first synthesized and then used to prepare the thiourea derivatives [4]. Benzoyl chloride has been reacted with ammonium thiocyanate in  $\text{CH}_2\text{Cl}_2$  solution under solid–liquid phase transfer catalysis, using

polyethylene glycol-400 as the catalyst, to give the corresponding benzoyl isothiocyanate. Dropwise addition of a solution of 1,4-butylenediamine in  $\text{CH}_2\text{Cl}_2$  yielded 3,3'-dibenzoyl-1,1'-(butane-1,4-diyl)dithiourea [5], while 3,3-bis(4-nitrophenyl)-1,10-(*p*-phenylene)dithiourea dimethylsulfoxide disolvate has been prepared by the reaction of (*p*-nitro)benzoyl isothiocyanate with *p*-phenylenediamine in  $\text{CH}_2\text{Cl}_2$  using polyethylene glycol-400 as a phase transfer catalyst [6]. This reaction has been carried using 1,6-hexyldiamine as the source of diamine to give *N,N*-(1,6-hexamethylene)-bis(benzoylthiourea) [7]. Thiocarbonohydrazide has been converted into 1-aminothiocarbamoyl-4-arylyl-3-thiosemicarbazides and 1,5-bis(arylylthiocarbamoyl) thiocarbonohydrazides by the addition of one or 2 mol of aroyl isothiocyanate, respectively. 1-Phenyl- or 1-benzylidene-thiocarbonohydrazide and aroyl isothiocyanates gave the appropriate mono-adducts analogously. 1-Aminothiocarbamoyl-4-benzoyl-3-thiosemicarbazide, the simplest representative of these classes of compounds, is cyclized to 3-mercapto-5-phenyl-1,2,4-triazole in alkaline media, and to 2-benzamido-5-mercapto-1,3,4-thiadiazole in acid media, the action of alkyl halides in the appropriate alcohol yields 2-benzamido-5-alkylthio-1,3,4-thiadiazoles [8]. The reaction of benzoyl isothiocyanate with *o*-phenylenediamine has been carried out in acetone using potassium thiocyanate as thiocyanate source [9].

In this work, the synthesis of some thiourea derivatives have

\* Corresponding author. Department of Basic Sciences, University of Health and Allied Sciences PMB 31, Ho, Ghana.

E-mail address: [felixessah15@gmail.com](mailto:felixessah15@gmail.com) (F. Odame).

been achieved by using ultrasound radiation, the compounds have been characterised using spectroscopy G C-MS and elemental analysis. The single crystal X-ray structure of *N*-[(benzyloxy) methanethioure] benzamide (**IV**), 1-benzoyl-3-(2-hydroxyethyl) thiourea (**V**) and 3-benzoyl-1-(1-benzyl piperidin-4-yl)thiourea (**VI**) have been presented and the bond lengths and bond angles contrasted with computed results. The HOMO and LUMO energy levels of the compounds have also been computed and discussed.

## 2. Experimental

### 2.1. Reagent and instrumentation

Analytical grade reagents and solvents for synthesis such as ammonium thiocyanate, 2-aminophenol, 3-aminophenol, 4-aminophenol, benzoyl alcohol, ethanolamine, 4-amino-*N*-benzylpiperidine were obtained from Sigma Aldrich (USA) whilst acetone and benzoyl chloride were obtained from Merck Chemicals (SA). The chemicals were used as received (i.e. without further purification). <sup>1</sup>H NMR and <sup>13</sup>C NMR spectra were recorded on a Bruker Avance AV 400 MHz spectrometer operating at 400 MHz for <sup>1</sup>H and 100 MHz for <sup>13</sup>C using DMSO-*d*<sub>6</sub> as solvent and tetramethylsilane as internal standard. Chemical shifts are expressed in ppm. FT-IR spectra were recorded on a Bruker Platinum ATR Spectrophotometer Tensor 27. Elemental analyses were performed using a Vario Elementar Microcube ELIII. Melting points were obtained using a Stuart Lasec SMP30 whilst the masses were determined using an Agilent 7890A GC System connected to a 5975C VL-MS-C with electron impact as the ionization mode and detection by a triple-axis detector. The GC was fitted with a 30 m × 0.25 mm × 0.25 μm DB-5 capillary column. Helium was used as carrier gas at a flow rate of 1.63 mL min<sup>-1</sup> with an average velocity of 30.16 cm s<sup>-1</sup> and a pressure of 63.73 kPa.

### 2.2. Conventional I method for the synthesis benzoyl isothiocyanate

Ammonium thiocyanate (0.01 mol, 0.76 g) was dissolved in 20 mL of acetone. Benzoyl chloride (0.01 mol, 1.13 mL) was added followed by heating under reflux at 100–120 °C for 2 h. The product was filtered, the respective amine or alcohol added and heated under reflux for 3 h. GC-Mass spectra were recorded for the synthesized compounds and they showed molecular ion (M<sup>+</sup>) peaks, in addition to others, which confirmed the formation the products.

### 2.3. Method for the synthesis benzoyl isothiocyanate using ultrasound

Ammonium thiocyanate (0.010 mol, 0.76 g) was dissolved in 20 mL of acetone. Benzoyl chloride (0.010 mol, 1.13 mL) was added followed by heating under reflux at 100–120 °C for 2 h. The product was filtered, the solvent removed, and the respective amine or alcohol added, 1 mL of acetone was then added and subjected to ultrasonic radiation for 60 min at room temperature. GC-Mass spectra were recorded for the synthesized compounds and they showed molecular ion (M<sup>+</sup>) peaks, in addition to others, which confirmed the formation the products.

#### 2.3.1. Optimimization of the reaction conditions for ultrasound method

Table 1 gives the optimization of the reaction conditions for the ultrasound method. The product or yields of the products have been given.

#### 2.3.2. 3-Benzoyl-1-(3-hydroxyphenyl)thiourea (**I**)

3-Aminophenol was added to benzoyl isothiocyanate, in 1 mL of

**Table 1**  
Optimization of reaction conditions for ultrasound method and their yields.

Compound	Solvent	Temperature	product/% yield	Time (minutes)
<b>I</b>	None	25	oily liquid	10
<b>1</b>	None	25	oily liquid	20
<b>1</b>	None	25	oily liquid	30
<b>1</b>	None	25	oily liquid	40
<b>1</b>	1 mL acetone	25	oily semi-solid	50
<b>1</b>	1 mL acetone	25	90	60
<b>II</b>	1 mL acetone	25	92	60
<b>III</b>	1 mL acetone	25	91	60
<b>IV</b>	1 mL acetone	25	86	60
<b>V</b>	1 mL acetone	25	89	60
<b>VI</b>	1 mL acetone	25	86	60

acetone and subjected to ultrasonic radiation for 60 min at room temperature. The product was redissolved in acetone, recrystallized and obtained as a light brown solid from DMSO:toluene (4:1). Yield = 90% (ultra sound), 75% (conventional method). Mp = 109–111 °C. <sup>1</sup>H NMR (ppm): 12.60 (s, 1H), 11.60 (s, 1H), 9.68 (s, 2H), 7.99 (d, 2H, *J* = 7.6 Hz), 7.65 (t, 1H, *J* = 6.8, 7.20 Hz), 7.54 (t, 2H, *J* = 7.2 Hz), 7.30 (s, 1H), 7.21 (t, 1H, *J* = 7.2, 8.0 Hz), 7.06 (d, 1H, *J* = 7.6 Hz), 6.70 (d, 1H, *J* = 8.0 Hz), <sup>13</sup>C NMR (ppm): 178.3 (C=S), 168.3 (C=O), 157.6 (C-N), 138.8 (Ph-H), 133.2 (Ph-H), 132.2 (Ph-H), 129.5 (Ph-H), 128.4 (Ph-H), 114.5 (Ph-H), 113.4 (Ph-H), 110.9 (Ph-H), 40.3. IR (ν<sub>max</sub>, cm<sup>-1</sup>): 3109 (N-H), 2810 (C-H), 1669 (C=O), 1593 (C=C), 1527 (C=C), 1446 (C-N), 1334 (C-O). Anal. calcd. for C<sub>14</sub>H<sub>12</sub>N<sub>2</sub>O<sub>2</sub>S: C, 61.75; H, 4.44; S, 11.77; N, 10.29. Found: C, 61.68; H, 4.38; S, 11.69; N, 10.29. LRMS (*m/z*, M<sup>+</sup>): Found for C<sub>14</sub>H<sub>12</sub>N<sub>2</sub>O<sub>2</sub>S = 272.25, Expected mass = 272.32.

#### 2.3.3. 3-Benzoyl-1-(2-hydroxyphenyl)thiourea (**II**)

2-Aminophenol was added to benzoyl isothiocyanate in 1 mL of acetone and subjected to ultrasonic radiation for 60 min at room temperature. The product was recrystallized and obtained as a yellow solid from DMSO:toluene (4:1). Yield = 92% (ultra sound) 73% (conventional method), Mp = 184–186 °C. <sup>1</sup>H NMR (ppm): 12.98 (s, 1H), 11.40 (s, 1H), 10.37 (s, 1H), 8.58 (d, 1H, *J* = 8.0 Hz), 7.97 (d, 2H, *J* = 7.20 Hz), 7.64 (t, 1H, *J* = 7.20 Hz), 7.53 (t, 2H, *J* = 7.20 Hz), 7.11 (t, 1H, *J* = 7.60 Hz), 7.00 (d, 1H, *J* = 8.0 Hz) and 6.88 (t, 1H, *J* = 7.2, 7.60 Hz). <sup>13</sup>C NMR (ppm): 177.6 (C=S), 168.3 (C=O), 148.9 (C-N), 133.1 (Ph-H), 132.1 (Ph-H), 128.6 (Ph-H), 126.4 (Ph-H), 125.9 (Ph-H), 123.2 (Ph-H), 118.4 (Ph-H), 115.1 (Ph-H). IR (ν<sub>max</sub>, cm<sup>-1</sup>): 3290 (N-H), 3011 (C-H), 1657 (C=O), 1557 (C=C), 1461 (C-N), 1373 (C-N), 1338 (C-O). Anal. calcd. for C<sub>14</sub>H<sub>12</sub>N<sub>2</sub>O<sub>2</sub>S: C, 61.75; H, 4.44; S, 11.77; N, 10.29. Found: C, 61.68; H, 4.38; S, 11.69; N, 10.29. LRMS (*m/z*, M<sup>+</sup>): Found for C<sub>14</sub>H<sub>12</sub>N<sub>2</sub>O<sub>2</sub>S = 272.25, Expected mass = 272.32.

#### 2.3.4. 3-Benzoyl-1-(4-hydroxyphenyl)thiourea (**III**)

4-Aminophenol was added to benzoyl isothiocyanate in 1 mL of acetone and subjected to ultrasonic radiation for 60 min at room temperature. The product was recrystallized and obtained as a light brown solid from DMSO: toluene (4:1). Yield = 91% (ultra sound) 72% (conventional method), Mp = 109–111 °C. <sup>1</sup>H NMR (ppm): 12.43 (s, 1H), 11.43 (s, 1H), 9.62 (s, 1H), 7.98 (d, 2H, *J* = 7.2 Hz), 7.65 (s, 1H), 7.55 (t, 2H, *J* = 7.2, 7.6 Hz), 7.43 (d, 2H, *J* = 8.0 Hz), 6.80 (d, 2H, *J* = 7.6 Hz), <sup>13</sup>C NMR (ppm): 178.9 (C=S), 168.3 (C=O), 155.8 (C-N), 132.9 (Ph-H), 129.2 (Ph-H), 128.4 (Ph-H), 125.8 (Ph-H), 115.1 (Ph-H). IR (ν<sub>max</sub>, cm<sup>-1</sup>): 3145 (N-H), 3000 (C-H), 1665 (C=O), 1598 (C=C), 1545 (C=C), 1456 (C-N), 1412 (C-N), 1323 (C-O). Anal. calcd. for C<sub>14</sub>H<sub>12</sub>N<sub>2</sub>O<sub>2</sub>S: C, 61.75; H, 4.44; S, 11.77; N, 10.29. Found: C, 61.68; H, 4.38; S, 11.69; N, 10.29. LRMS (*m/z*, M<sup>+</sup>): Found for C<sub>14</sub>H<sub>12</sub>N<sub>2</sub>O<sub>2</sub>S = 272.25, Expected mass = 272.32.

### 2.3.5. *N*-[(benzyloxy)methanethioly]benzamide (**IV**)

Benzyl alcohol was added to benzoyl isothiocyanate in 1 mL of acetone and subjected to ultrasonic radiation for 60 min at room temperature. The product was recrystallized and obtained as a pale-yellow solid from DMSO: toluene (4:1). Yield = 86% (ultra sound) 70% (conventional method), Mp = 67–68 °C, <sup>1</sup>H NMR (ppm): 12.09 (s, 1H), 7.90 (d, 2H, *J* = 7.6 Hz), 7.60 (t, 1H, *J* = 7.2 Hz), 7.48 (m, 4H), 7.40 (m, 3H), 5.60 (s, 2H), <sup>13</sup>C NMR (ppm): 189.2 (C=S), 165.3 (C=O), 135.0 (Ph-H), 133.0 (Ph-H), 128.4 (Ph-H), 127.9 (Ph-H), 72.2 (CH<sub>2</sub>), IR ( $\nu_{\max}$ , cm<sup>-1</sup>): 3307 (N-H), 3244 (N-H), 1710 (C=O), 1692 (C=O), 1601 (C=C), 1514 (C=C), 1489 (C-N), 1455 (C-N), 1373 (C-O). Anal. calcd. for C<sub>15</sub>H<sub>13</sub>NO<sub>2</sub>S: C, 66.40; H, 4.83; S, 11.82; N, 5.16. Found: C, 66.32; H, 4.76; S, 11.79; N, 5.11. LRMS (*m/z*, M<sup>+</sup>): Found for C<sub>15</sub>H<sub>13</sub>NO<sub>2</sub>S = 271.28, Expected mass = 271.33.

### 2.3.6. 1-Benzoyl-3-(2-hydroxyethyl)thiourea (**V**)

Ethanolamine was added to benzoyl isothiocyanate in 1 mL of acetone and subjected to ultrasonic radiation for 60 min at room temperature. The product was recrystallized and obtained as a colourless solid from DMSO:toluene (4:1). Yield = 89% (ultra sound) 71% (conventional method), Mp = 114–116 °C, <sup>1</sup>H NMR (ppm): 11.26 (s, 1H), 11.04 (s, 1H), 7.92 (d, 2H, *J* = 7.2 Hz), 7.63 (t, 1H, *J* = 7.2 Hz), 7.56 (t, 2H, *J* = 7.6 Hz), 5.05 (s, 1H), 3.04 (m, 4H), <sup>13</sup>C NMR (ppm): 180.3 (C=S), 168.0 (C=O), 132.9 (Ph-H), 132.3 (Ph-H), 128.4 (Ph-H), 58.4 (CH<sub>2</sub>), 47.5 (CH<sub>2</sub>). IR ( $\nu_{\max}$ , cm<sup>-1</sup>): 3322 (N-H), 3224 (N-H), 2947 (C-H), 1668 (C=O), 1602 (C=C), 1525 (C=C), 1300 (C-O). Anal. calcd. for C<sub>10</sub>H<sub>12</sub>N<sub>2</sub>O<sub>2</sub>S: C, 53.55; H, 5.39; S, 14.30; N, 12.49. Found: C, 53.48; H, 5.33; S, 14.25; N, 12.42. LRMS (*m/z*, M<sup>+</sup>): Found for C<sub>10</sub>H<sub>12</sub>N<sub>2</sub>O<sub>2</sub>S = 224.22, Expected mass = 224.28.

### 2.3.7. 3-Benzoyl-1-(1-benzylpiperidin-4-yl)thiourea (**VI**)

4-Amino-*N*-benzylpiperidine was added to benzoyl isothiocyanate in 1 mL of acetone and subjected to ultrasonic radiation for 60 min at room temperature. The product was recrystallized and obtained as a light brown solid from DMSO:toluene (4:1). Yield = 86% (ultra sound) 76% (conventional method) Mp = 112–114 °C. <sup>1</sup>H NMR (ppm): 10.95 (s, 1H), 7.91 (d, 2H, *J* = 7.6 Hz), 7.60 (t, 1H, *J* = 7.2 Hz), 7.50 (s, 2H), 7.30 (s, 4H), 7.24 (m, 1H), 4.22 (s, 1H), 3.47 (s, 2H), 2.65 (m, 2H), 2.17 (t, 2H), 1.97 (m, 2H), 1.58 (q, 2H, C(5)-H). <sup>13</sup>C NMR (ppm): 178.9 (C=S), 168.2 (C=O), 138.2 (Ph-H), 133.0 (Ph-H), 131.9 (Ph-H), 128.8 (Ph-H), 128.5 (Ph-H), 128.4 (Ph-H), 128.1 (Ph-H), 127.1 (Ph-H), 62.0 (CH<sub>2</sub>), 51.0 (CH<sub>2</sub>), 30.0 (CH<sub>2</sub>). IR ( $\nu_{\max}$ , cm<sup>-1</sup>): 3229 (N-H), 2980 (C-H), 1725 (C=O), 1654 (C=O), 1509 (C=C), 1164 (C-N). Anal. calcd. for C<sub>20</sub>H<sub>23</sub>N<sub>3</sub>O<sub>2</sub>S: C, 67.96; H, 6.56; S, 9.07; N, 11.89. Found: C, 67.90; H, 6.52; S, 9.02; N, 11.82. LRMS (*m/z*, M<sup>+</sup>): Found for C<sub>20</sub>H<sub>23</sub>N<sub>3</sub>O<sub>2</sub>S = 353.42, Expected mass = 353.48.

## 2.4. X-ray crystal structure determination

X-ray diffraction analyses of **IV**, **V** and **VI** were performed at 200 K using a Bruker Kappa Apex II diffractometer with monochromated Mo K $\alpha$  radiation ( $\lambda$  = 0.71073 Å). APEXII [10], was used for data collection and [11], for cell refinement and data reduction. The structures were solved by direct methods using SHELXS-2013 [10] and refined by least-squares procedures using SHELXL-2013 [11], with SHELXL [10], as a graphical interface. All non-hydrogen atoms were refined anisotropically. Carbon-bound H atoms were placed in calculated positions (C-H 0.95 Å for aromatic carbon atoms and C-H 0.99 Å for methylene groups) and were included in the refinement in the riding model approximation, with Uiso (H) set to 1.2Ueq (C). The H atoms of the methyl groups were allowed to rotate with a fixed angle around the C-C bond to best fit the experimental electron density (HFIX 137 in the SHELX program suite [11]) with Uiso (H) set to 1.5Ueq (C). Nitrogen-bound H atoms

were located on a difference Fourier map and refined freely. Data were corrected for absorption effects using the numerical method implemented in SADABS [12].

## 2.5. Computational studies

The calculations were carried out using the Gaussian 09 program [13]. Molecular geometries of the singlet ground state of all the compounds were fully optimized in the gas phase at the density functional theory (DFT) level of theory using hybrid B3LYP [14–16], B3PW91, and wB97XD functionals together with the 6-31G (d,p) basis set.

The B3LYP functional has been used in computing vibrational frequencies, NMR, MEP, by Mulliken population analysis (MPA), Hirshfeld population analysis (HPA) and Natural population analysis (NPA) schemes as well as computation of thione-thiol isomers [17–19].

For compound **I** a frequency calculation was carried out to ensure that the optimized molecular structure corresponded to a minimum [20], thus only positive frequencies were expected. The HOMO and LUMO results as well as the information for bond length and bond angles were obtained using Avogadro.

## 3. Results and discussion

### 3.1. Synthesis

The different amine derivatives were added to benzoyl isothiocyanate and subjected to ultrasonic radiation for 60 min at room temperature. Scheme 1 gives the synthetic schemes for the synthesis of compounds **I-VI**.

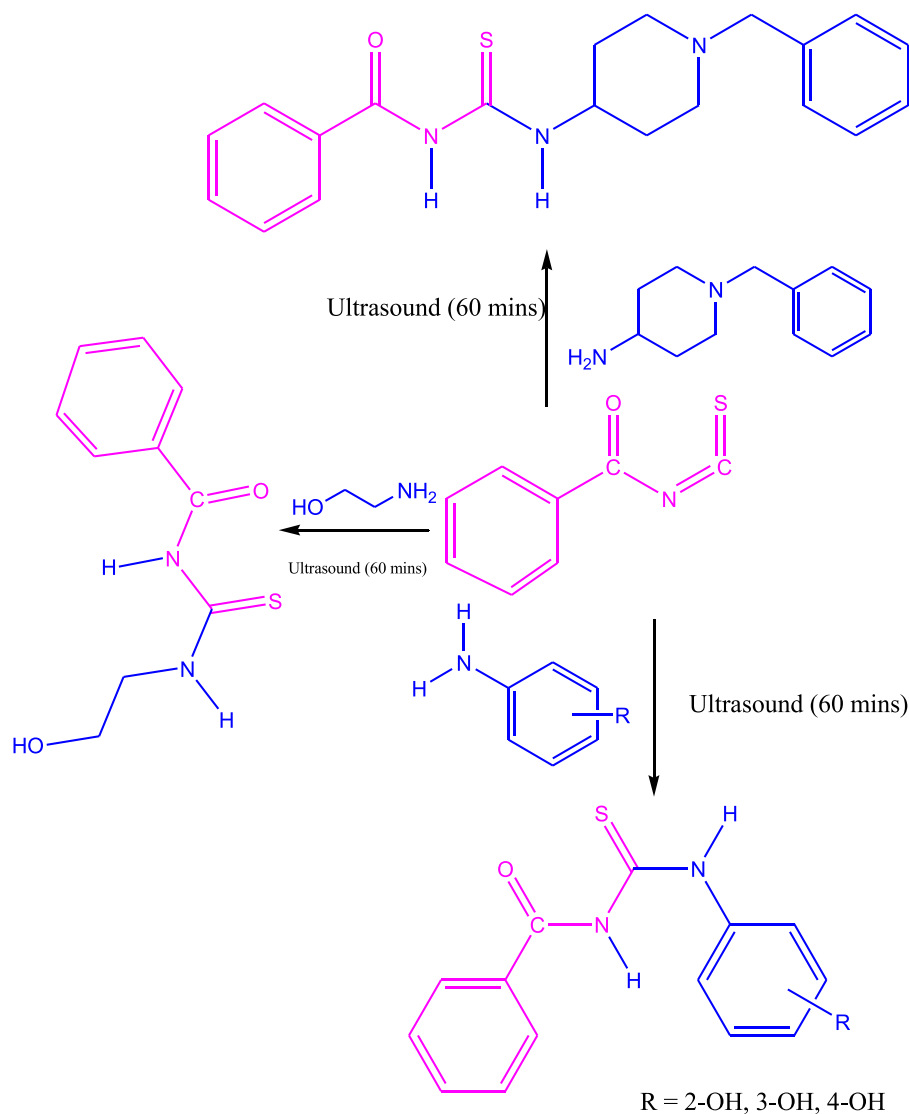
### 3.2. Spectroscopic characterization

Signals for the N-H proton were observed between 12.98 and 10.37 ppm. Aromatic protons gave signals between 8.58 and 6.80 ppm, whilst aliphatic protons gave signals between 3.04 and 1.97 ppm. In the <sup>13</sup>C NMR spectrum the thione signal was observed between 180.3 and 177.6 ppm whilst the carbonyl occurred between 168.3 and 161.0 ppm. Signals for aromatic carbons were observed between 157.6 and 148.9 ppm. Aliphatic carbon signals were observed between 58.4 and 40.3 ppm. The IR spectrum gave signals for the N-H stretch between 3322 and 3109 cm<sup>-1</sup>, which is within the range reported for N-H of thiones [21]. The N-H signal for compound **I** coincides with the broad OH signal hence signal suppression could account for the low NH value of 3109 cm<sup>-1</sup>. The aliphatic C-H stretch occurred between 2980 and 2810 cm<sup>-1</sup>. The C=O stretch of a carbonyl was observed between 1783 and 1710 cm<sup>-1</sup> and between 1669 and 1654 cm<sup>-1</sup> whilst the C=C stretch was observed between 1598 and 1525 cm<sup>-1</sup>.

Table 2 gives the list of synthesized compounds and their yields.

### 3.3. Crystal structures of compounds **IV**, **V** and **VI**

Compounds **IV**, **V** and **VI** were recrystallized from DMSO:Toluene (1:1). Compound **IV** was obtained as a pale yellow solid, whilst compounds **V** and **VI** were obtained as colourless and light brown solids respectively. The crystallographic data, selected experimental and computed bond lengths and bond angles for the crystal structures of compounds **IV**, **V** and **VI** are provided in Tables 3, 4, 5 and 6. The ORTEP diagrams for compounds **IV**, **V** and **VI** are presented in Figs. 1–3. Compound **IV** crystallized in the orthorhombic space group *Iba*2, whilst compounds **V** and **VI** crystallized in the monoclinic space group *P21/c* (see Table 5) (see Table 6).



**Scheme 1.** Synthesis of thiourea derivatives.

In compound **IV** the bond distances O1–C1 and O2–C4 are 1.222(2) and 1.424(2) which are consistent with carbonyls [22], whilst the bond distances of S1–C2 which is 1.674(1) is typical of thiones [23]. The bond angles of S1–C2–N2 and S1–C2–N1 are 124.8(1) and 118.9(1) respectively this confirms the carbon atoms are  $sp^2$  hybridized. The bond distances of O1–C1, O1–C2 and O2–C3 in compound **V** are 1.462(2), 1.316(2) and 1.213(2) Å for a carbonyl. The bond angles of S1–C2–O1 and S1–C2–N1 were 126.5(1) and 121.0(1)° respectively. Whilst compound **VI** gave the bond distances 1.6733(1), 1.225(2) and 1.373(2) Å for S1–C2, O1–C1 and N1–C1 respectively.

The computed bond lengths for compounds **IV**, **V** and **VI** using the B3LYP, CAM-B3LYP, B3PW91, WB97XD and M06 functionals and the 6–311 g (p,d) basis set gave deviations of between 0.001 and 0.168 Å. The computed bond lengths of S1–C2 for compound **IV** yielded deviations of between 0.002 and 0.012 Å from the experimentally determined bond lengths of compound **IV** which was 1.646(2) Å. The computed carbonyl bond lengths of O1–C1 and O1–C2 gave deviations between 0.009 and 0.033 Å from the experimental values of 1.462(2) and 1.316(2) Å. The computed amide bonds of N1–C3 and N1–C2 gave deviations between 0.002

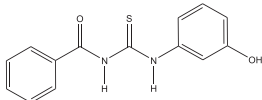
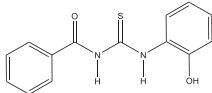
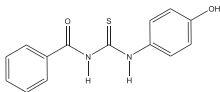
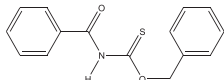
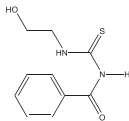
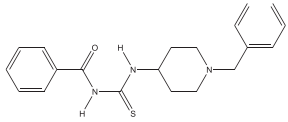
and 0.022 from the experimentally obtained values of 1.383(2) and 1.377(2) respectively.

The computed C1–C11 and C3–C21 bond lengths gave deviations of between 0.001 and 0.013 from the experimentally determined values of 1.493(3) and 1.491(2). The bond angles of C1–O1–C2, C2–N1–C3 and O1–C1–C11 were obtained from experiment as 119.5(1), 129.0(2) and 105.9(2)° respectively whilst the computed values gave deviations between 0.1 and 1.5°. The experimentally determined bond angles of S1–C2–O1 and S1–C2–N1 were 126.5(1) and 121.0(1)° respectively whilst the computed values gave deviations between 0.6 and 7.2°. The large deviations which only occurred in these angles might be due the fact gas phase considerations in computations are different from the measurement obtained from the single crystal structure.

The bond length of S1–C2 bond for compound **V** was experimentally determined as 1.674(1)° whilst the computed bond length gave deviations between 0.001 and 0.005 Å from the experimental values. For the amide bonds N1–C1, N1–C2, N2–C2 and N2–C3 the experimental bond lengths obtained were 1.374(2), 1.393(2), 1.321(2) and 1.456(2) Å respectively, the computed values deviated by 0.001 and 0.012 from the experimental values.

**Table 2**

List of synthesized compounds and their yields.

Compound	Structure	% yield Ultrasound promoted	% yield (conventional)
I		90	75
II		92	73
III		91	72
IV		86	70
V		89	71
VI		86	76

**Table 3**

Crystallographic data and structure refinement summary for compounds IV, V and VI.

Property	IV	V	VI
Formula	C <sub>15</sub> H <sub>13</sub> NO <sub>2</sub> S	C <sub>10</sub> H <sub>12</sub> N <sub>2</sub> O <sub>2</sub> S	C <sub>20</sub> H <sub>23</sub> N <sub>3</sub> OS
CCDC Number	1540945	1540946	1540947
Formula Weight	271.32	224.28	353.47
Crystal System	Orthorhombic	Monoclinic	Monoclinic
Space group	<i>Iba</i> 2	P2 <sub>1</sub> /c	P2 <sub>1</sub> /c
a [Å]	16.8239(6)	17.0904(12)	13.5447(6)
b [Å]	17.0617(6)	4.5028(4)	12.5136(6)
c [Å]	9.5096(3)	14.2120(13)	11.0282(4)
α [°]	90	90	90
β [°]	90	102.079(4)	100.177(2)
γ [°]	90	90	90
V [Å <sup>3</sup> ]	2729.68(16)	1069.47(16)	1839.79(14)
Z	8	4	4
D(calc) [g/cm <sup>3</sup> ]	1.320	1.393	1.276
Mu(MoKa) [1/mm]	0.234	0.284	0.189
F(000)	1136	472	752
Crystal Size [mm]	0.15 × 0.29 × 0.60	0.22 × 0.25 × 0.30	0.15 × 0.23 × 0.30
Temperature (K)	200	200	200
Radiation [Å]	MoKa 0.71073	MoKa 0.71073	MoKa 0.71073
Theta Min-Max [°]	1.7, 28.3	2.4, 28.4	2.2, 28.3
Dataset	−22: 21; −22: 22; −12: 12	−22: 22; −5: 4; −18: 18	−18: 18; −16: 15; −14: 14
Tot., Uniq. Data, R(int)	12557, 3398, 0.018	9982, 2633, 0.019	17817, 4573, 0.029
Observed Data [I > 2.0 sigma(I)]	3231	2123	3398
Nref	3398	2633	4573
Npar	177	145	234
R	0.0287	0.0352	0.0384
wR <sub>2</sub>	0.0736	0.0927	0.1021
S	1.03	1.04	1.01
Max. and Av. Shift/Error	0.00, 0.00	0.00, 0.00	0.00, 0.00
Min. and Max. Resd. Dens. [e/Å <sup>3</sup> ]	−0.32, 0.17	−0.24, 0.31	−0.22, 0.31

The bond lengths of O1–C1 and O2–C4 were experimentally determined as 1.222(2) and 1.424(2)° whilst the computed values

gave deviations of between 0.002 and 0.014° representing the lowest deviations from the computed values. The bond angles of

**Table 4**  
Summary of theoretical and experimental bond lengths and bond angles of N-[(benzyloxy)methanethioly]benzamide (IV) using B3LYP, CAM-B3LYP, B3PW91, WB97XD and M06 functionals and 6–311 g(d,p) basis set.

Bond length (Å)								
Compound IV								
Experimental	B3LYP	CAM-B3LYP	B3PW91	WB97XD	M06	Min Deviation	Max Deviation	
S1–C2	1.646(2)	1.644	1.634	1.637	1.636	1.634	0.002	0.012
O1–C1	1.462(2)	1.453	1.442	1.444	1.438	1.434	0.009	0.028
O1–C2	1.316(2)	1.349	1.340	1.345	1.338	1.341	0.022	0.033
N1–C3	1.383(2)	1.405	1.398	1.400	1.378	1.400	0.005	0.022
N1–C2	1.377(2)	1.383	1.377	1.379	1.397	1.379	0.002	0.02
C1–C11	1.493(3)	1.502	1.498	1.499	1.500	1.492	0.001	0.009
C3–C21	1.491(2)	1.504	1.500	1.500	1.500	1.496	0.005	0.013
C11–C12	1.389(3)	1.399	1.391	1.396	1.392	1.389	0.002	0.01
O2–C3	1.213(2)	1.206	1.200	1.204	1.181	1.200	0.007	0.032
Bond Angles (°)								
Experimental	B3LYP	CAM-B3LYP	B3PW91	WB97XD	M06	Min Deviation	Max Deviation	
C1–O1–C2	119.5(1)	119.2	119.4	118.6	119.1	118.8	0.1	0.9
C2–N1–C3	129.0(2)	129.8	129.4	129.6	129.2	129.2	0.2	0.8
O1–C1–C11	105.9(2)	107.3	107.2	107.4	107.3	107.4	1.3	1.5
O1–C2–N1	112.5(2)	106.0	106.1	106.1	106.1	106.0	6.4	6.5
S1–C2–O1	126.5(1)	125.9	125.7	125.8	125.9	125.9	0.8	0.6
S1–C2–N1	121.0(1)	128.1	128.2	128.0	128.1	128.1	7.0	7.2
O2–C3–N1	123.8(2)	123.9	123.9	124.1	122.3	124.1	0.3	1.5
O2–C3–C21	120.4(2)	122.4	122.3	122.5	123.9	122.5	2.0	3.5
N1–C3–C21	115.7(1)	113.6	113.7	113.5	113.7	113.3	2.0	2.4
C1–C11–C12	121.4(2)	120.5	120.5	120.5	120.5	120.9	0.5	0.9

**Table 5**  
Summary of theoretical and experimental bond lengths (Å), and bond angles (°) for 1-benzoyl-3-(2-hydroxyethyl)thiourea (V) using B3LYP, CAM-B3LYP, B3PW91, WB97XD and M06 functionals and 6–311 g(d,p) basis set.

Bond length (Å)								
Compound V								
EXPERIMENTAL	B3LYP	CAM-B3LYP	B3PW91	WB97XD	M06	Min Deviation	Max Deviation	
S1–C2	1.674(1)	1.682	1.673	1.674	1.673	1.669	0.001	0.005
O1–C1	1.222(2)	1.224	1.217	1.222	1.217	1.216	0.002	0.006
O2–C4	1.424(2)	1.426	1.418	1.417	1.415	1.410	0.002	0.014
N1–C1	1.374(2)	1.382	1.375	1.377	1.377	1.379	0.001	0.008
N1–C2	1.393(2)	1.405	1.399	1.400	1.399	1.400	0.006	0.012
N2–C2	1.321(2)	1.333	1.326	1.331	1.331	1.331	0.005	0.012
N2–C3	1.456(2)	1.454	1.449	1.447	1.448	1.445	0.002	0.011
C1–C11	1.493(2)	1.498	1.495	1.494	1.497	1.491	0.002	0.005
C3–C4	1.511(2)	1.517	1.511	1.513	1.513	1.505	0.002	0.006
C11–C12	1.378(2)	1.400	1.393	1.397	1.395	1.393	0.015	0.022
Bond Angles (°)								
EXPERIMENTAL	B3LYP	CAM-B3LYP	B3PW91	WB97XD	M06	Min Deviation	Max Deviation	
S1–C2–N2	124.8(1)	126.3	126.1	126.4	126.0	126.0	1.2	1.6
C1–N1–C2	128.0(1)	129.3	129.0	129.2	129.1	129.3	1.0	1.3
O1–C1–N1	122.5(1)	122.9	123.0	123.0	123.2	123.3	0.4	0.8
O2–C4–C3	108.0(1)	107.3	107.1	107.4	107.4	107.3	0.6	0.9
C2–N2–C3	123.9(1)	124.3	124.0	124.1	123.8	123.3	0.1	0.6
N1–C1–C11	116.1(1)	115.5	115.5	115.4	115.2	115.6	0.5	0.9
O1–C1–C11	121.5(1)	121.6	121.5	121.6	121.6	121.7	0.1	0.2
N1–C2–N2	116.3(1)	115.9	116.0	115.8	116.0	115.8	0.3	0.5
S1–C2–N1	118.9(1)	117.7	117.8	117.8	118.1	118.2	0.7	1.1
N2–C3–C4	111.4(1)	109.6	109.2	109.8	109.1	109.2	1.8	2.3

C1–N1–C2, O1–C1–N1 and O2–C4–C3 were experimentally determined as 128.0(1), 122.5(1) and 108.0(1)° whilst the computed values gave deviations of between 0.4 and 1.3°.

The bond length of S1–C2 bond for compound VI was experimentally determined as 1.673(1)° whilst the computed bond length gave deviations between 0.054 and 0.065 Å from the experimental

values. For the amide bonds N1–C1, N1–C2, N2–C2 and N2–C3 the experimental bond lengths obtained were 1.373(2), 1.398(2), 1.320(2) and 1.465(2) Å respectively, the computed values deviated by 0.041 and 0.168 Å from the experimental values. The bond lengths of C1–C11 and C3–C31 were experimentally determined as 1.492(2) and 1.507(2)° whilst the computed values gave deviations

**Table 6**

Summary of theoretical and experimental bond lengths (Å), and bond angles (°) for 3-benzoyl-1-(1-benzylpiperidin-4-yl)thiourea (VI) using B3LYP, CAM-B3LYP, B3PW91, WB97XD and M06 functionals and 6-311 g(d,p) basis set.

Bond length (Å)								
Compound VI								
Experimental	B3LYP	CAM-B3LYP	B3PW91	WB97XD	M06	Min Deviation	Max Deviation	
S1–C2	1.673(1)	1.619	1.608	1.614	1.610	1.610	0.054	0.065
O1–C1	1.225(2)	1.199	1.194	1.198	1.195	1.193	0.026	0.032
N1–C1	1.373(2)	1.453	1.439	1.444	1.439	1.446	0.066	0.08
N1–C2	1.398(2)	1.357	1.355	1.354	1.357	1.354	0.041	0.044
N2–C2	1.320(2)	1.490	1.490	1.481	1.475	1.486	0.155	0.17
N2–C23	1.465(2)	1.303	1.295	1.302	1.297	1.298	0.162	0.168
N21–C21	1.465(2)	1.450	1.447	1.446	1.446	1.445	0.015	0.02
N21–C25	1.468(2)	1.452	1.445	1.444	1.444	1.442	0.016	0.026
C1–C11	1.492(2)	1.483	1.482	1.480	1.483	1.476	0.009	0.016
C3–C31	1.507(2)	1.514	1.509	1.509	1.509	1.501	0.002	0.007
Bond Angles (°)								
Experimental	B3LYP	CAM-B3LYP	B3PW91	WB97XD	M06	Min Deviation	Max Deviation	
C1–N1–C2	127.0(1)	126.3	125.9	126.2	126.1	125.7	0.1	0.6
N2–C23–C24	110.9(1)	119.9	120.0	119.9	120.3	120.3	9.0	9.4
C2–N2–C23	123.9(1)	126.5	125.7	126.2	125.4	124.9	1.0	2.3
C3–N21–C21	110.4(1)	113.7	113.2	113.6	113.0	112.3	0.9	3.3
N21–C25–C24	112.3(1)	109.7	109.7	109.9	109.7	109.8	2.4	2.6
S1–C2–N2	124.8(1)	132.2	132.0	132.0	131.8	132.6	7.0	7.8
S1–C2–N1	118.8(1)	117.6	118.1	117.6	118.6	117.8	0.2	1.2
N1–C2–N2	116.4(1)	110.3	109.9	110.3	109.6	109.6	6.1	6.8
C3–N21–C25	107.5(1)	113.6	113.2	113.6	113.1	112.0	4.5	6.1

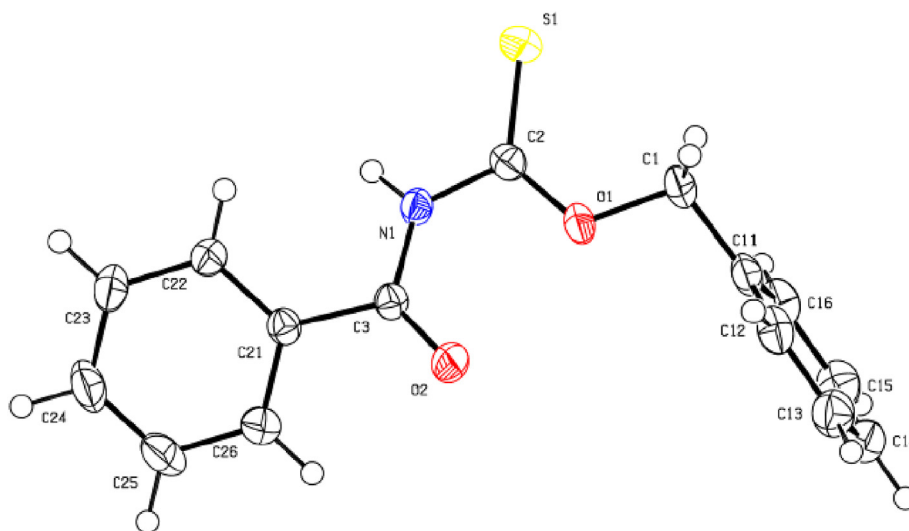


**Fig. 1.** An ORTEP view of *N*-[(benzyloxy)methanethioyl]benzamide (IV) showing 50% probability displacement ellipsoids and the atom labelling

of between 0.002 and 0.016° representing the lowest deviations from the computed values. The bond angles of C2–N2–C23, C3–N21–C21 and N21–C25–C24 were experimentally determined as 123.9(1), 110.4(1) and 112.3(1)° whilst the computed values gave deviations of between 0.9 and 3.3°.

### 3.5. Chemical reactivity

The HOMO and LUMO are the determinants of chemical stability of any species [24,25]. The HOMO is associated with the ability to donate an electron whilst the LUMO is associated with the ability to accept an electron. The energy of the HOMO determines the ionization potential whilst the energy of the LUMO determines the

electron affinity. The energy difference between HOMO and LUMO orbitals, known as the energy gap, determines the stability or reactivity of molecules [26]. The energy gap determines the electrical conductivity of the compound [27]. The lower the energy gap the higher the conductivity and vice versa. The hardness of a molecule also corresponds to the gap between the HOMO and LUMO orbitals [28].

The energy gap ( $E_{\text{HOMO}} - E_{\text{LUMO}}$ ) is an important stability index used to characterize the chemical reactivity and kinetic stability of the molecule [29]. A molecule with a small energy gap is more polarized and reactive because it easily offer electrons to an acceptor. Low energy gap values may be due to conjugation [30]. The energies of frontier molecular orbitals, energy band gap

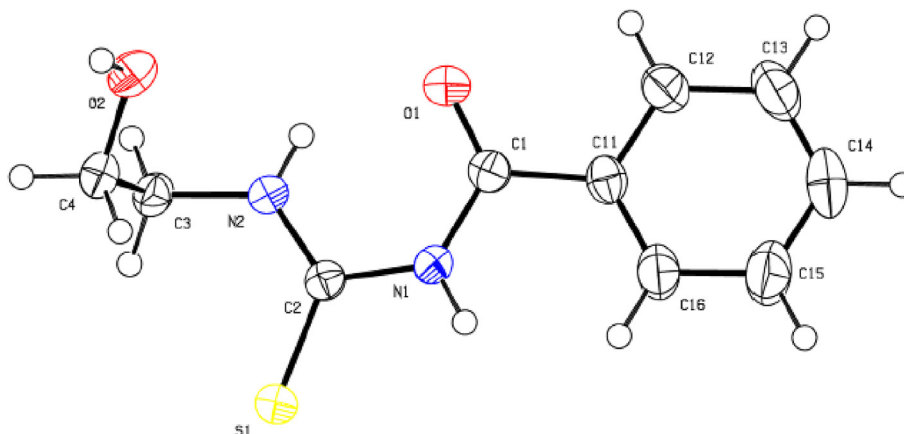


Fig. 2. An ORTEP view of 1-benzoyl-3-(2-hydroxyethyl)thiourea (V) showing 50% probability displacement ellipsoids and the atom labelling.

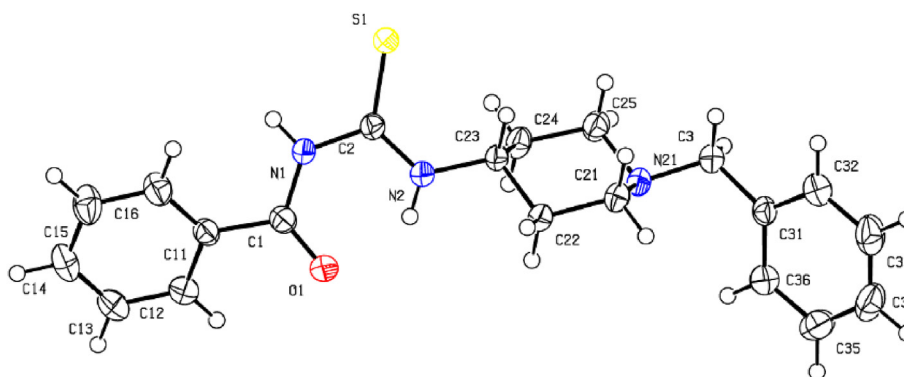


Fig. 3. An ORTEP view of 3-benzoyl-1-(1-benzylpiperidin-4-yl)thiourea (VI), showing 50% probability displacement ellipsoids and the atom labelling.

( $E_{\text{HOMO}}-E_{\text{LUMO}}$ ), electronegativity ( $\chi$ ), chemical potential ( $\mu$ ), global hardness ( $\eta$ ), global softness ( $S$ ) and global electrophilicity index ( $\omega$ ) all contribute to the reactivity of the molecule concerned. It is found that stability of molecules related to hardness [31]. Electronegativity is the power of an atom in a molecule to attract electron to it-self [32]. The electrophilicity index gives a measure of energy lowering due to highest electron transfer between donor and acceptor [33]. The electrophilicity is a descriptor of reactivity that allows a quantitative classification of the global electrophilic nature of a molecule within a relative scale. To understand the toxicity of various pollutants in terms of their reactivity and site selectivity, the new reactivity quantity can be demonstrated [34,35].

The HOMO–LUMO energy levels of compounds *N*-[(benzyloxy) methanethiyl]benzamide (IV) using b3lyp, cam-b3lyp, b3pw91, wb97xd and m06 functionals and 6–311 g(d,p) basis set is given by Table S1. The HOMO and LUMO for compound (IV) gave energy gaps of between 0.15136 and 0.30026 eV. The high energy gap is consistent with its high melting point and low solubility in most solvents [36].

The HOMO and LUMO gave energy gaps of between 0.14786 and 0.29369 eV. The high energy gap is consistent with its high melting point and low solubility in most solvents. Whilst Tables S2 and S3 gives the HOMO–LUMO energy levels of compound (V) and (VI) respectively. The HOMO and LUMO gave energy gaps of between 0.10670 and 0.25105 eV. The high energy gap is consistent with its

high melting point and low solubility in most solvents. Tables S4–S6 gives the global reactivity descriptors for compounds IV, V and VI using b3lyp, cam-b3lyp, b3pw91, wb97xd and m06 functionals and 6–311 g(d,p) basis set. Of the three compounds, VI gave the highest computed electronegativities of between 0.2844 and 0.28895 eV, whilst compounds IV and V gave comparably lower values. Compound VI therefore has a greater tendency to attract electrons to itself. Whilst it has a lower chemical potential for the same reason. All three compounds have comparable global hardness and global softness, whilst compound VI has a higher global electrophilicity index than compound IV and V which is consistent with its high electronegativity.

Tables S7–S9 gives the comparison of the computed NMR with experimental data. The  $^1\text{H}$  NMR computation are mostly in good agreement with the experimental results except the amided protons whilst the  $^{13}\text{C}$  NMR are inconsistent.

### 3.6. Molecular electrostatic potential analysis

In the computation of the molecular electrostatic potential for compounds IV to VI two conformations were obtained for each compound. Tables S10–S12 gives the collated molecular electrostatic maps for the two conformers of compounds IV to VI. The various charged regions are represented by different colours. The blue colour represents the positive region and it is prone to nucleophilic attack the red colour represents the negative region

and so electrophilic attack.

### 3.7. Interpretation of vibrational spectra

Fig. S4 gives the plot of computed IR spectra for two conformations A and B of **IV**. The scaling factors used were 0.921 (b3lyp), 0.908 (cam-b3lyp), 0.916 (b3pw91), 0.908 (wb97xd) and 0.920 (m06). The values obtained were compared to reported values 0.967 (b3lyp/6-311G(d,p)), 0.963 (b3pw91/6-311G(d,p)) and 0.957 (wb97xd/6-311G(d,p)). Key experimental bands at 3307/3244  $\text{cm}^{-1}$  (a, N–H), 1710/1692  $\text{cm}^{-1}$  (b, C=O) and 1455  $\text{cm}^{-1}$  (c, N–H) are shown as vertical markers in Fig. S4. Whilst Fig. S5 gives the plot of computed IR spectra for two conformations A and B of **V**. The scaling factors used were 0.932 (b3lyp), 0.923 (cam-b3lyp), 0.928 (b3pw91), 0.919 (wb97xd) and 0.930 (m06). The computed values were compared to reported values 0.967 (b3lyp/6-311G(d,p)), 0.963 (b3pw91/6-311G(d,p)) and 0.957 (wb97xd/6-311G(d,p)). Key experimental bands at 3322/3224  $\text{cm}^{-1}$  (a, N–H), 1668/1602  $\text{cm}^{-1}$  (b, C=O) and 1300  $\text{cm}^{-1}$  (c, N–H) are shown as vertical markers in Fig. S5. The plot of computed IR spectra for two conformations A and B of **VI** is given by Fig. S6. The scaling factors used were 0.935 (b3lyp), 0.920 (cam-b3lyp), 0.931 (b3pw91), 0.915 (wb97xd) and 0.99 (m06). Compare reported values 0.967 (b3lyp/6-311G(d,p)), 0.963 (b3pw91/6-311G(d,p)) and 0.957 (wb97xd/6-311G(d,p)). Key experimental bands at 3229  $\text{cm}^{-1}$  (a, N–H), 1725/1654  $\text{cm}^{-1}$  (b, C=O) and 1509  $\text{cm}^{-1}$  (c, N–H) are shown as vertical markers in Fig. S6.

## 4. Conclusion

Synthesis of some thiourea derivatives have been achieved by using ultrasound, the compounds have been characterised using IR, NMR, GC-MS and elemental analysis. The single crystal X-ray diffraction analysis of *N*-[(benzyloxy)methanethiyl]benzamide (**IV**), 1-benzoyl-3-(2-hydroxyethyl)thiourea (**V**) and 3-benzoyl-1-(1-benzylpiperidin-4-yl)thiourea (**VI**) has been presented and the bond lengths and bond angles contrasted with computed results. The HOMO and LUMO energy levels of the compounds have also been computed and discussed. The chemical reactivity descriptors of compounds **IV–VI** have been computed and discussed. Two conformers were obtained for compounds **IV** to **VI** in the molecular Electrostatic potential and the vibrational frequency computations and these have been discussed.

### Declaration of competing interest

We have no competing financial interest or personal relationships which may be considered as potential competing interest.

### CRediT authorship contribution statement

**Felix Odame:** Validation, Formal analysis, Investigation, Data curation, Writing - original draft, Visualization, Project administration. **Eric C. Hosten:** Data curation. **Zenixole Tshentu:** Resources, Writing - review & editing, Supervision, Funding acquisition.

### Acknowledgements

F. Odame thanks the National Research Foundation of South Africa for awarding him a postdoctoral Fellowship. The authors would like to acknowledge the Centre for High Performance

Computing in South Africa for the use of their computing resources (CHEM0864).

## Appendix A. Supplementary data

Supplementary data to this article can be found online at <https://doi.org/10.1016/j.molstruc.2020.128302>.

## Supplementary Material

Supplementary data associated with this article can be found, in the online version. CCDC number, **1540945**, **1540946** and **1540947** contain the crystal structures associated with this article.

## References

- [1] T.J. Peglow, G.P. da Costa, L.F.B. Duarte, M.S. Silva, T. Barcellos, G. Perin, D. Alves, *J. Org. Chem.* 84 (9) (2019) 5471–5482.
- [2] J.S. Ghomi, M.A. Ghasemzadeh, *J. Serb. Chem. Soc.* 76 (5) (2011) 679–684.
- [3] J.S. Ghomi, M. Tavazo, *Ultrason. Sonochem.* 40 (2018) 230–237.
- [4] R. Mohebat, G. Mohammadian, *J. Chem. Res.* 36 (11) (2012) 626–628.
- [5] Y.J. Ding, X.B. Chang, X.Q. Yang, W.K. Dong, *Acta Crystallogr. E64* (2008) o658.
- [6] W.K. Dong, H.B. Yan, L.Q. Chai, Z.W. Lv, C.Y. Zhao, *Acta Crystallogr. E64* (2008) o1097.
- [7] W.K. Dong, X.Q. Yang, L. Xu, L. Wang, G.L. Liu, J.H. Feng, *Z. Kristallogr. NCS 222* (2007) 279–280.
- [8] F. Kurzer, *J. Chem. Soc. (C)* (1971) 2932–2938.
- [9] S.K. Kang, N.S. Cho, M.K. Jeon, *Acta Crystallogr. E68* (2012) o395.
- [10] APEX2 SADABS, SAINT, Bruker AXS Inc, Madison, WI, USA, 2010.
- [11] G.M. Sheldrick, A short history of SHELX, *Acta Crystallogr. A* 64 (2008) 112–122.
- [12] C.B. Hübschle, G.M. Sheldrick, B. Dittrich, *ShelXle: J. Appl. Crystallogr.* 44 (2011) 1281–1284.
- [13] M.J. Frisch, G.W. Trucks, H.B. Schlegel, G.E. Scuseria, M.A. Robb, J.R. Cheeseman, J.A. Montgomery, T. Vreven, K.N. Kadin, J.C. Burant, J.M. Millam, S.S. Iyengar, J. Tomasi, V. Barone, B. Mennucci, M. Cossi, G. Scalmani, N. Rega, G.A. Petersson, H. Nakatsuji, M. Hada, M. Hears, K. Toyota, R. Fukuda, J. Hasegawa, M. Ishida, T. Nakajima, Y. Honda, O. Kitao, H. Nakai, M. Klene, X. Li, J.E. Knox, H.P. Hratchian, J.B. Cross, V. Bakken, C. Adamo, J. Jaramillo, R. Gomperts, R.E. Stratmann, O. Yazyev, A.J. Austin, R. Cammi, C. Pomelli, J.W. Ochterski, P.Y. Ayala, K. Morokuma, G.A. Voth, P. Salvador, J.J. Dannenberg, V.G. Zakrzewski, S. Dapprich, A.D. Daniels, M.C. Strain, O. Farkas, D.K. Malick, A.D. Rabuck, K. Raghavachari, J.B. Foresman, J.V. Ortiz, Q. Cui, A.G. Baboul, S. Clifford, J. Cioslowski, B.B. Stefanov, G. Liu, A. Liashenko, P. Piskorz, I. Komaromi, R.L. Martin, D.J. Fox, T. Keith, M.A. Al-Laham, C.Y. Peng, A. Nanayakkara, M. Challacombe, P.M.W. Gill, B. Johnson, W. Chen, M.W. Wong, C. Gonzalez, J.A. Pople, Gaussian Inc., Pittsburgh, 2003.
- [14] P.C. Hariharan, J.A. Pople, *Theor. Chim. Acta* 28 (1973) 213–322.
- [15] P.C. Hariharan, J.A. Pople, *Mol. Phys.* 27 (1974) 209–214.
- [16] W. Kohn, A.D. Becke, R.G. Parr, *J. Phys. Chem.* 100 (1996) 12974–12980.
- [17] R. Joshi, N. Pandey, S.K. Yadav, R. Tilak, H. Mishra, S. Pokharia, *J. Mol. Struct.* 1164 (15) (2018) 386–403.
- [18] J.N. Ghogomu, N.K. Nkungli, *Adv. Chem.* 15 (2016), 9683630.
- [19] Z. Kazeminejad, A. Shiroudil, K. Pourshamsian, F. Hatamjafari, A.R. Oliaey, *J. Chil. Chem. Soc.* (64) (2019), No 1.
- [20] A. Frisch, A.B. Nielson, A.J. Holder, GAUSSVIEW User Manual, Gaussian Inc., Pittsburgh, 2000.
- [21] F.H. Jumaa1, N.O. Tapabashi, O.A. Abd, Synthesis and characterization of some 5, 5-ethyl bis- (4-amino-4H-1, 2, 4-triazole-3thiol) derivatives, *J. Sci. Eng. Res.* 4 (2017), 8 98–106.
- [22] F. Odame, E. Hosten, R. Betz, K. Lobb, Z.R. Tshentu, *Acta Chim. Slov.* 62 (2015) 986–994.
- [23] F. Odame, E.C. Hosten, Z.R. Tshentu, R. Betz, *Z. Kristallogr. NCS 229* (2014) 337–338.
- [24] V. Choudhary, A. Bhatt, D. Dash, N. Sharma, DFT calculations on molecular structures, HOMO-LUMO study, reactivity descriptors and spectral analyses of newly synthesized diorganotin(IV) 2-chloridophenylacetohydroxamate complexes, *J. Comput. Chem.* 40 (27) (2019) 2354–2363.
- [25] P. Matunová, V. Jirásek, B. Rezek, DFT calculations reveal pronounced HOMO-LUMO spatial separation in polypyrrole-nanodiamond systems, *Phys. Chem. Chem. Phys.* 21 (2019) 11033–11042.
- [26] L. Padmaja, R.C. Kunar, D. Sajan, I.H. Joe, V.S. Jayakumar, G.R. Pettit, O.F. Nielsen, *J. Raman Spectrosc.* 40 (2009) 419–428.
- [27] A. Poiyamozi, N. Sundaraganesan, M. Karabacak, O. Tanrıverdi, M. Kurt, *J. Mol. Struct.* 1024 (2012) 1–12.

- [28] P. Udhayakala, A. Jayanthi, T.V. Rajendiran, S. Gunasekaran, Arch. Appl. Sci. Res. 3 (4) (2011) 424–439.
- [29] M. Govindarajan, S. Periandy, K. Carthigayen, Spectrochim. Acta A 97 (2012) 411–422.
- [30] G.M. Abu El-Reash, O.A. El-Gammal, S.E. Ghazy, A.H. Radwan, Spectrochim. Acta A 104 (2013) 26–34.
- [31] R.G. Parr, P.K. Chattaraj, J. Am. Chem. Soc. 113 (1991) 1854–1855.
- [32] L. Pauling, The Nature of the Chemical Bond, third ed., Cornell University Press, Ithaca, New York, 1960.
- [33] R.G. Parr, L.V. Szentpaly, S. Liu, J. Am. Chem. Soc. 121 (1999) 1922–1924.
- [34] R. Parthasarathi, J. Padmanabhan, V. Subramanian, B. Maiti, P.K. Chattaraj, J. Phys. Chem. 107 (2003) 10346–10352.
- [35] R. Parthasarathi, J. Padmanabhan, V. Subramanian, B. Maiti, P.K. Chattaraj, Curr. Sci. 86 (2004) 535–542.
- [36] J. Aihara, Reduced HOMO–LUMO gap as an index of kinetic stability for polycyclic aromatic hydrocarbons, J. Phys. Chem. A 103 (37) (1999) 7487–7495.